Quantifying the Diffusion of a Fluid through Membranes by Remote Detection MRI

Ville-Veikko Telkki,[1,2]* C. Hilty,[1,3] S. Garcia,[1] E. Harel,[1] and A. Pines[1]

[1]Materials Sciences Division, Lawrence Berkeley National Laboratory, and Department of Chemistry, University of California at Berkeley, Berkeley, California 94720-1460, USA

[2] NMR Research Group, Department of Physical Sciences, University of Oulu, P. O. Box 3000, FIN-90014 University of Oulu, Finland

[3] Now at: Department of Chemistry, Texas A&M University, College Station, Texas 77842, USA

*To whom correspondence should be addressed. E-mail: telkki@waugh.cchem.berkeley.edu

One sentence summary: The diffusion rate of a fluid across thin porous membrane sheets is determined by a new type of remote detection magnetic resonance imaging (MRI) method with high sensitivity and without pressure or concentration gradients.

Abstract:

We present a method to measure self-diffusion across membranes without the need for concentration or pressure gradients. Hyperpolarized xenon in combination with remote detection of NMR allows the measurement of membrane permeation, even in the gas phase. The resulting images allow quantification of the amount of fluid diffused through the membrane, and represent an alternative, potentially more precise way of measuring a membrane diffusion coefficient. The use of remote detection of NMR allows for non-invasive signal encoding coupled to sensitive detection, making this approach ideal for the study of diffusion in intact devices such as fuel cells or separation systems.

Membranes are of paramount importance in science and technology, for example for fuel cells (*1*), for the purification of water (*2*), gas separation (*3*), or metabolism (*4*). Present methods for the characterization of diffusion across membranes typically rely on the determination of the change in concentration or partial pressure of the fluid in a system which is in non-equilibrium at the beginning of the measurement. Alternatively, radio-active nuclei that are incorporated into the diffusing compounds are sometimes used as tracers. (*5*) However, the dependence of the diffusion coefficient on concentration may lead to results that differ from the equilibrium values, whereas in the latter case the labeling is often chemically challenging and the difference in mass between labeled and unlabeled molecule may affect results. (*5*)

Here, we present direct, spatially localized measurement of membrane permeability by magnetic resonance imaging (MRI). Uniquely, this MRI method allows the observation of transport of molecular species across the membrane under equilibrium conditions by encoding the spatial position of molecules onto their nuclear spin states, and then localizing them for a second time after transport has occurred. The equilibrium measurement allows for a simplified, time-independent physical model, reducing the number of parameters and increasing precision. In this study, we employ xenon to characterize the gas diffusion properties of two inorganic aluminum oxide membranes. Xenon is frequently used for characterizing porous media (*6*), and allows for hyperpolarization to boost the obtainable NMR signal (*7*,*8*). We demonstrate that by employing hyperpolarization of xenon in combination with remote detection of NMR, it is possible to increase sensitivity to a level that allows the measurement of gas

permeation through a membrane. Due to higher spin density in liquids, this method of remote detection of NMR will also be applicable to the determination of their diffusion properties without hyperpolarization.

A conventional NMR experiment uses the same coil for the encoding of spin coherences and for the detection of the signal, requiring a compromise of optimal parameters for each step. Remote detection of NMR spatially separates the encoding and detection steps. (*9*) The flow of a probe fluid transports the signal from the sample region to the detector. This method increases the signal-to-noise ratio (SNR) of NMR experiments by means of separate optimization of the encoding and detection while providing time-of-flight (TOF) information of the fluid molecules as they flow from the encoding region to the detector that reveals the flow paths and the dispersion. (*10 -13*) The information contained in the remotely detected flow images is determined by its encoding sequence, which in the present case consists of two phase encoded imaging steps that are separated in time. This allows direct quantification of the amount of substance that has diffused through the membrane during the time between these two steps.

Two different ANOPORE^{TM} inorganic aluminum oxide membranes containing straight, parallel pores with the pore axis perpendicular to the surface of the membrane were studied. (*14*) The pore diameters of the membranes were 20 and 200 nm, and the thickness of both membranes was 60 μm. In the measurements, the membrane was set in the center along the long axis of a channel with square cross section. The gas mixture containing hyperpolarized xenon gas flowed parallel to its surface with equal pressure on

both sides of the membrane (Fig. 1A). Subsequently, the gas flowed into an outlet tube, and through the NMR detection coil. (*15*)

In order to determine the flow rate and dispersion of the gas in the sample, z encoded TOF images (*10*) were measured from the sample. The experiment began with a π/2 radio frequency (rf) pulse followed by the labeling of spin coherences by a magnetic field gradient pulse in the z direction. The coherences were then stored as longitudinal magnetization by applying another π/2 rf pulse. The amplitude of the encoded z magnetization was read stroboscopically by a series of π/2 rf pulses in the detection coil.

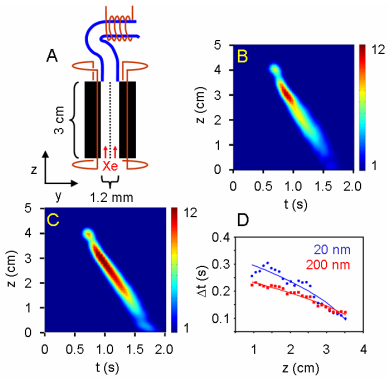

Fig. 1. (A) Schematic of the holder containing the square flow channel inside the encoding coil. The detection coil was wrapped around the outlet tubing. Gas flow is from bottom to top. (B) and (C) z encoded TOF images for the membranes containing (B) 20 nm and (C) 200 nm pores. (D) The width Δt of the TOF curve as a function of z position for both membranes (pore sizes are shown in the figure). The solid lines represent least squares fits of dispersion curves described in the text to the data points.

The TOF images (Figs. 1B and 1C) show that the atoms located close to the outlet of the channel (z = 3.5 cm) during the encoding step arrive first in the detection coil, and that TOF increases linearly with increasing distance to the detection coil. The non-linearity of the TOF curve above z = 3.5 cm is a consequence of a narrowing in the flow channel at

the point where the gas arrives in the outlet tubing. These images were used to calibrate and adjust the flow rate of the gas. On the basis of the slopes in the membrane region, it can be calculated that the flow rate in these two experiments was 3.93 ± 0.07 and 3.85 ± 0.06 cm/s for the 20 and 200 nm pore membranes, respectively. The values show that the flow rate was very stable in different experiments.

Because of hydrodynamic dispersion of the fluid atoms, the width of the TOF curves increases with increasing distance from the detection coil (Fig. 1D). At the long diffusion time limit, the mean square displacement, Δz^2, due to hydrodynamic dispersion is $\Delta z^2 \approx 2Kt + \Delta z_0^2$ (*10,16*), where K is a dispersion coefficient and Δz_0^2 is the displacement at the sample outlet. Δz^2 can be calculated from the time-domain full-width-at-half-maximum, Δt, as $\Delta z^2 = (v\Delta t)^2/(8\ln 2)$. By fitting the dispersion curve to the values measured from the TOF images, it was observed that K is about double for the 20 nm membrane (0.17 ± 0.02 cm^2/s) as compared to the 200 nm membrane (0.090 ± 0.004 cm^2/s). K can be taken as a measure of the fluid retention inside of the membrane.

Extension of the previous TOF imaging experiment to two spatial dimensions by applying encoding gradients in two different orthogonal directions gives more detailed insight into the flow. (*10*) Weak intensity in the middle of the channel in the time projections of yz encoded TOF images (Fig. 2) shows that the membranes indeed split the channel into two sub-channels. The Reynolds number in the sub-channels is very low (about 40), indicating laminar flow. However, because the diffusion of gas across the sub-channel (20 ms for 0.5 mm) is fast compared with the travel times, the average TOF

does not depend on the lateral position of the gas atoms during the encoding. The image intensity in the individual panels therefore does not show the otherwise expected curved flow profile. Above the end of the membrane region (z = 3.5 cm), the gas begins to flow coherently in the undivided channel, and no intensity gap is seen anymore in the center of the channel. The narrowing of the flow channel in that region can also be seen from the flow profile.

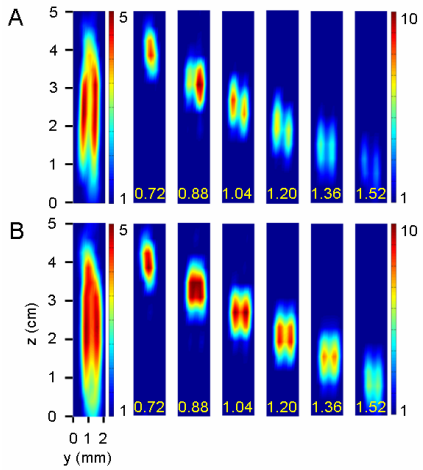

Fig. 2. yz encoded TOF images for the membranes containing (A) 20 nm and (B) 200 nm pores. The left hand side pictures are time projections. The other images are the averages of the measurements of three successive travel times. The average travel time in seconds is shown in the panels.

From the yz encoded TOF images it is not obvious whether xenon atoms pass through the pores or not because of the weak intensity in the membrane region. However, the lateral movement of gas atoms can be revealed by adding a second y encoding step, separated from the first one by a small delay. As the spin state is preserved between the two phase encoding steps, they allow correlation of the initial position with the final position of an ensemble of fluid atoms. The pulse sequence for this double y (yy) encoded TOF experiment is shown in Fig. 3A. The first two rf pulses and the gradient pulse between

them represent the first encoding step including the storage of one component of the magnetization in the longitudinal direction in order to prevent dephasing during the delay τ. The delay is followed by the second phase encoding step, after which the magnetization is stored again as longitudinal magnetization. Subsequently, the fluid flows to the detector, and the amplitude of the longitudinal magnetization modulated by both encoding steps is detected by a train of π/2 pulses in the same way as in previous remote detection experiments. In order to obtain quadrature detection in each dimension and to destroy the signal of unecoded atoms, a 16-step phase cycling of the pulses is applied in the experiment. (*14*)

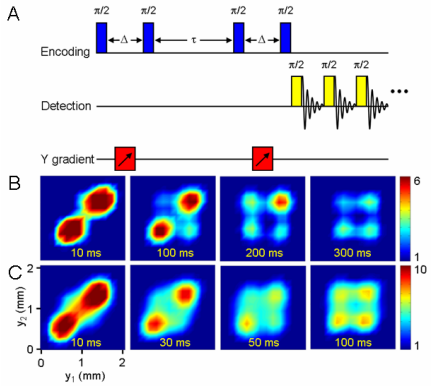

Fig. 3. The pulse sequence of the yy encoded experiment (A) and y correlation images measured for the membranes containing (B) 20 nm and (C) 200 nm pores. The delays τ used in the experiments are shown in the images.

Figs. 3B and 3C show the correlations between the y values of y_1 and y_2 in the first and second encoding steps, respectively, obtained from the yy encoded TOF experiments. The intensity of any [y_2, y_1] pixel in the image is proportional to the probability of an atom to be situated in an xz slice at y_1 during the first encoding step and in the slice at y_2 during the second step. In the images, 10 successive transients of TOF measurement were

summed in order to increase the SNR. The transients were selected so that the images contain signal only from the membrane region (between z = 0.5 and 3.5 cm).

In the case of the shortest delay (τ = 10 ms), a diagonal pattern is observed, indicating that the diffusion through the membrane is insignificant during τ. However, the rounded spots close to the corners of the images show that significant diffusion across the sub-channels takes place during the delay. When τ is increased, off-diagonal peaks (cross peaks) begin to grow, evidencing transport of xenon gas through the membrane. The amplitude of the cross peaks increases more rapidly with increasing τ for the 200 nm membrane than for the 20 nm membrane.

The normalized amplitude a_{cross} of the cross peaks (normalization: $a_{diag} + a_{cross} = 1$, where a_{diag} is the amplitude of diagonal peaks) represents the portion of xenon gas diffused through the membrane during the delay τ. On the basis of Fick's law of diffusion, it can be derived that the amplitudes of diagonal and cross peaks behave as a function of τ as $a_{diag} = 1/2 * (1 + \exp(-2D\tau / w_s t_m))$ and $a_{cross} = 1/2 * (1 - \exp(-2D\tau / w_s t_m))$, where D is a diffusion constant of xenon inside the membrane, and w_s and t_m are width of the sub-channel (0.6 mm) and the thickness of the membrane (60 μm), respectively. (*14*) The least-squares adjustment of these curves to the integrated amplitudes (Fig. 4) results in D values of $(1.54 \pm 0.07)*10^{-7}$ m^2/s for the 20 nm membrane and $(7.5 \pm 0.2)*10^{-7}$ m^2/s for the 200 nm membrane.

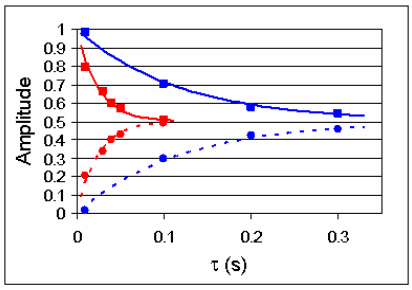

Fig. 4. Amplitudes of diagonal (squares) and cross (circles) peaks of the samples containing 20 (blue) and 200 nm (red) pores. Solid and dashed lines are least squares adjustments of the equations for diagonal and cross peaks, respectively, to the data points, as described in the text.

It has been shown that a yy encoded remotely detected TOF experiment can be used for the quantitative analysis of diffusion through a membrane without the need for pressure or concentration gradients. A corresponding experiment can also be done in a conventional way by detecting the signal using the encoding coil immediately after the last gradient pulse. However, it can be estimated that in the present setup, using a 3 cm encoding and a 2 mm detection coil, the SNR per unit time is about 20 times larger in the remotely detected experiment because of the much more sensitive detection coil with better filling factor. (*14*) Because the yy encoded remote detection experiment takes about two hours, the direct experiment with the same SNR would take about one month, which is unfeasible. Even though in the present experiment, a somewhat smaller encoding coil could have been used, the membrane assembly will always require a certain amount of space. A larger coil allows for an increased experimental flexibility in particular when working with intact technological devices. In addition, remote detection uniquely provides TOF information that can be used to determine the axial dispersion of the fluid flow, as a measure of fluid retention inside of the membrane, and for selecting signal only from the membrane region of the sample.

In the present experiment, both phase encoding steps were done in the y direction, but in principle more detailed information could be obtained by three dimensional phase encoding, or even with an added chemical shift dimension. In practice, sensitivity and experiment time should be weighed against the additional information obtained in determining the level of complexity of the encoding sequence. The use of hyperpolarized xenon takes advantage both of the high signal obtained from hyperpolarization and of the long spin-lattice relaxation time of xenon. This approach allows comparison of diffusion properties among different membranes. In cases where the diffusion properties of a specific analyte are of interest, the presented method is also applicable especially for substances in the liquid state which yield a strong NMR signal due to the higher spin density. Any spin-carrying nucleus that is present in a gas or a liquid of interest can in principle be used for this experiment, as long as the diffusion time is shorter than the spin-lattice relaxation time. This NMR method is maximally non-invasive because it does not require the introduction of foreign tracers, and molecular interactions and transport of the molecules under study do not depend on the nuclear spin state.

Especially substances in the liquid state yield a stronger NMR signal, even without hyperpolarization, due to the higher spin density of a liquid. Any spin-carrying nucleus that is present in a gas or a liquid of interest can in principle be used for this experiment, as long as the diffusion time is shorter than the spin-lattice relaxation time. If an intrinsically present nucleus is used, the NMR method is maximally non-invasive because it does not require the introduction of foreign tracers, and molecular interactions and transport of the molecules under study do not depend on the nuclear spin state.

MRI allows for the spatial encoding of fluid in any geometry, thus for example enabling the measurement of localized properties of the sample. Apart from enabling the diffusion measurements without any pressure or concentration gradients, such a scheme can be used for correlating the transport of fluid between any points in the encoding region, giving detailed insight into the flow paths. Due to the use of non-invasive MRI encoding, combined with the highly sensitive remote detection of the signal, this experiment should allow characterizing membrane diffusion and transport in intact systems of technological importance, such as fuel cells and gas separation systems. In a broader context, the presented scheme is also the first remote detection experiment that uses a more elaborate encoding step than simple spatial or frequency encoding. It demonstrates the wide applicability of remote detection in general. Experiments of this specific type will not only be applicable to measure diffusion across membranes, but also to characterize different flow regimes such as laminar flow or turbulence, as well as to study flow in porous media.

1. K. Kordesch, G. Simader, *Fuel Cells and Their Applications* (VCH, New York, 2001).
2. R. Singh, *Hybrid Membrane Systems for Water Purification* (Elsevier, Oxford, 2006).
3. W. R. Vieth, *Diffusion in and through Polymers* (Hanser Verlag, Munich, 1991).
4 M. Höfer, *Transport Across Biological Membranes* (Pitman Publishing, Marshfield, 1981).
5. J. Crank, G. S. Park, Eds., *Diffusion in Polymers* (Academic Press, New York, 1968).
6. C.I. Ratcliffe, *Annu. Rep. NMR Spectrosc.* **36** 123 (1998).
7. T. G. Walker, W. Happer, *Rev. Mod. Phys*. **69**, 629 (1997).
8. B. M. Goodson, *J. Magn. Reson*. **155**, 157 (2002).
9. A. J. Moule *et al.*, *Proc. Natl. Acad. Sci. U.S.A.* **100**, 9122 (2003).
10. J. Granwehr, E. Harel, S. Han, S. Garcia, A. Pines, *Phys. Rev. Lett.* **95**, 075503 (2005).
11. E. Harel, J. Granwehr, J. Seeley, A. Pines, *Nature Materials* **5**, 321 (2006).
12. C. Hilty *et al.*, *Proc. Nat. Acad. Sci. U.S.A.* **102**, 14960 (2005).
13. S. Xu *et al*., *Proc. Natl. Acad. Sci. U.S.A.* **103** 12668 (2006).
14. Materials and methods are available as supporting material on *Science* Online.
15. E. E. McDonnell, S. Han, C. Hilty, K. L. Pierce, A. Pines, *Anal. Chem*. **77**, 8109 (2005).
16. G. I. Taylor, *Proc. R. Soc. A* **219**, 186 (1953).

Supporting Online Material for

Quantifying the Diffusion of a Fluid through Membranes by Remote Detection MRI

Ville-Veikko Telkki,* C. Hilty, S. Garcia, E. Harel, and A. Pines

*To whom correspondence should be addressed. E-mail:

telkki@waugh.cchem.berkeley.edu

Published XXX

DOI: XXX

This PDF includes:

Experimental

ANOPORE^{TM} inorganic aluminum oxide membranes were manufactured by Structure Probe Inc (West Chester, PA). The membrane under study was set in the center of a channel with square cross section, parallel to its axis. Xenon gas flowed on both sides parallel to the membrane. The details of the sample holder are shown in Fig. S1.

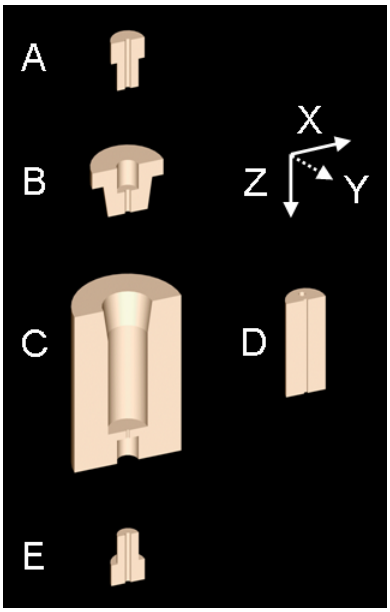

Fig. S1. A cross-section of the membrane holder. 1/16" O.D. tubing was connected with a fitting (A) to a plug (B), which was screwed into the actual sample holder (C). Height and diameter of the holder were 5 and 3 cm, respectively. The holder contained a cylindrical chamber, and the membrane was placed along the center axis of the chamber, squeezed in between two half cylinders (D) (length 3 cm, diameter 1.1 cm). The flow channel was milled into the flat surfaces of the half cylinders. Gas flowed through a small hole from the chamber to a fitting connecting to tubing with 1/16" O.D. (E). The tubing led to detection coil. A cross-section of the channel is shown in Fig. 1A. The width of the square flow channel was about 1.2 mm, with the membrane placed in the middle of the channel in the xz plane. Hyperpolarized xenon gas flowed in the z direction, and diffusion of xenon gas through the membrane was measured in the y direction.

In the remote detection experiments, the encoding was done by a commercial imaging probe (Varian inc, Palo Alto) with a cylindrical cavity (3 cm in diameter) along its full length (4 cm). A home built detection probe was pushed from underneath into the cavity so that the detection coil was about 1.5 cm below the imaging coil region. The detection

coil was wrapped around 1/16” O.D. outlet tubing, and the length of the coil was about 5 mm. The rf isolation between the two probes was achieved with a grounded copper shield. More information about the design of the auxiliary probe can be found from ref. (*S1*). The NMR experiments were performed on a Unity Inova 300 MHz spectrometer (Varian inc), in which the xenon resonance frequency is 82.9 MHz.

The gas flowing through the sample was a mixture of Xe (1 %), N_2 (10 %), and He (89 %). The spin polarization of ^{129}Xe nuclei was optically enhanced to about 3 % using a commercial polarizer (Amersham Health, Durham, NC). The flow rate of the gas from the polarizer was adjusted to be about 0.3 standard liter per minute (SML) in order to obtain proper polarization. The flow was then divided into two branches after the polarizer in order to obtain slow enough flow rate through the actual sample. The flow rate and pressure at the outlet of the sample were controlled by a needle valve, with the pressure kept at about 5 atm. The flow rate and stability were monitored throughout the experiments by bubbling the gas from the sample through a small water column (7 mm diameter; 2 cm in length), using an outlet opening of 1/32”. The bubbles were detected with a fiber-optic counter which was interfaced via a digital input line to a computer that was running a LabView program to measure and log the bubble rate. Even though this measurement of the flow rate was not strictly quantitative, it proved to be an easy and robust method to ensure reproducibility in the experiments.

In the z encoded TOF experiments, the field of view (FOV) was 5 cm and the resolution was 2.1 mm (24 gradient steps). 32 transients were acquired in a total experiment time of 26 min.

In the yz encoded TOF experiments, the FOV in the y and z direction was 2.1 mm and 5 cm, respectively, and corresponding resolutions were 0.3 and 7.1 mm (7 gradient steps in both directions). The number of transients was 32 and total experiment time was 53 min.

In the yy encoded TOF experiments, the FOV of y_1 and y_2 was 2.1 mm and the resolution was 0.3 mm (7 gradient steps in both cases). The number of transients was 64 and total experiment time about 2 h. Values of the delay τ were 10, 100, 200 and 300 ms for the 20 nm membrane and 10, 30, 40, 50 and 100 ms for the 200 nm membrane.

In all the remote detection experiments, the acquisition time of one free induction decay (FID) was 40 ms (which is also the time resolution in TOF experiments), and 50 consecutive FID's were collected during one scan, leading to total acquisition time of 2 s per transient.

An alternative way for determining spatial correlations of flow of fluids is position exchange spectroscopy (POXSY), in which two encoding steps are set symmetrically inside a spin-echo pulse sequence. (*S2*) Even though it is originally planned for single coil experiment, it would be straightforward to implement in remotely detected way. However, in the case of relatively long delays between the encoding steps and between

the last encoding pulse and detection, it is advantageous to store the coherences as longitudinal magnetization as was done in the present experiment in order to avoid signal loss due to T_2 relaxation that arises from field inhomogeneities.

Phase cycling in yy encoded TOF experiment

In order to obtain quadrature detection (QD) in each dimension and to subtract the signal of unencoded spins, a specific phase cycling of the pulses is needed in the yy encoded experiment. An implementation is shown in Table S1. The phase cycle mimics a directly detected experiment in which a $\pi/2$ pulse is followed by the first and second encoding gradient and the signal detection without any delays and storage pulses; the same product operator terms are collected and summed together in the remote yy encoded experiment after applying the first four steps of the phase cycling scheme in the table, and this assures QD in each dimension. In addition, the phases of the second and fourth encoding pulses as well as the detection pulses are inverted in a proper way in order to remove the signal of unencoded atoms, which leads to 4*4 = 16 cycles altogether.

Table S1. 16-step phase cycling used in the yy encoded experiment. m is the cycle counter, ϕ_{enc1} refers to the phase of the first encoding pulse, ϕ_{enc2} to the second, etc., ϕ_{det} is the phase of all the detection pulses in one cycle, and ϕ_{rec} is the phase of receiver.

m	ϕ_{enc1}	ϕ_{enc2}	ϕ_{enc3}	ϕ_{enc4}	ϕ_{det}	ϕ_{rec}
0	x	x	x	x	x	x
1	x	x	x	y	x	x
2	x	y	x	x	x	x
3	x	y	x	y	x	x
4	x	-x	x	x	-x	x
5	x	-x	x	y	-x	x
6	x	-y	x	x	-x	x
7	x	-y	x	y	-x	x
8	x	x	x	-x	-x	x
9	x	x	x	-y	-x	x
10	x	y	x	-x	-x	x
11	x	y	x	-y	-x	x
12	x	-x	x	-x	x	x
13	x	-x	x	-y	x	x
14	x	-y	x	-x	x	x
15	x	-y	x	-y	x	x

Derivation of equations for the amplitudes of the signals in yy encoded TOF experiment

According to Fick's law, the rate of net diffusion (with pressure difference) is $D * A/t_m * \Delta P$, where D is the diffusion constant, A is the surface area of the membrane, t_m is the thickness of the membrane (60 μm in this case), and ΔP is the difference in partial pressure across the membrane. In this case, there is no pressure difference across the membrane. However, immediately after the first encoding step the concentration of xenon atoms encoded on one side of the membrane is zero on the other side, and therefore the rate can be modified for self-diffusion as $D * A/ t_m * C$, where C is the concentration of atoms encoded on the former side. We have two sub-channels, 1 and 2. Let $C_{ik}(\tau)$ be the concentration of atoms that were initially in sub-channel i, and that are in sub-channel k at time τ, and let w_s be the width of the sub-channel (0.6 mm). On the basis of the diffusion rates, the following equations can be derived: $dC_{11}/d\tau = D / w_s t_m * (-C_{11} + C_{12})$, $dC_{12}/d\tau = D / w_s t_m * (-C_{12} + C_{11})$, $dC_{21}/d\tau = D / w_s t_m * (-C_{21} + C_{22})$, and $dC_{22}/d\tau = D / w_s t_m * (-C_{22} + C_{21})$. At $\tau = 0$, $C_{11} = C_{22} = C$ and $C_{12} = C_{21} = 0$. Concentrations $C_{ik}(\tau)$ can be solved on the basis of previous equations, and because $a_{diag} \alpha C_{11} + C_{22}$ and $a_{cross} \alpha C_{12} + C_{21}$, after the normalization $a_{diag} + a_{cross} = 1$ we obtain $a_{diag} = 1/2 * (1 + \exp(-2D\tau / w_s t_m))$ and $a_{cross} = 1/2 * (1 - \exp(-2D\tau / w_s t_m))$.

Estimation of SNR ratio enhancement

Here we estimate the enhancement of the signal-to-noise ratio (SNR) in a remotely detected yy encoded TOF experiment when compared with a corresponding experiment detected by the encoding coil immediately after the last gradient pulse.

The theoretical sensitivity ratio of the detection and encoding coil is $\Lambda = t_{90}^{e} / t_{90}^{d} = 100$, where t_{90}^{e} and t_{90}^{d} are lengths of 90 degree pulses for encoding and detection coils, respectively. (*S3*) The volume of xenon gas in the encoding (V_e) and detection (V_d) region is about 40 mm^3 and 2.5 mm^3, respectively. Theoretical SNR enhancement of the signal measured directly by the coils is $\Lambda * V_d/V_e = 100 * 2.5/40 = 6.3$. The measured enhancement of the SNR is 6.9, which is in agreement with the theoretical enhancement.

Assuming that all the encoded xenon atoms are detected by optimizing the delay between detection pulses so that between the pulses all the atoms detected previously have left the detection coil volume, and the volume is filled by undetected atoms, the number of FID signals collected in a remote detection experiment is $V_e/V_d = 16$. If these signals are summed together, the SNR enhancement is $16^{1/2} * 6.9 = 27.6$. However, in the direct experiment QD detection for the second dimension is obtained inherently whereas in the remote detection version additional phase cycling is needed, which leads decrease of SNR enhancement by the factor of $2^{1/2}$. Therefore, the total theoretical SNR enhancement in yy encoded TOF experiment is about 20 as compared to the corresponding directly detected experiment.

In the previous calculation, the effect of dispersion, which decreases the obtained SNR enhancement, is neglected. On the other hand, choosing signal only from the membrane region of the sample can be done by time-of-flight in the remotely detected experiment, and it is more straightforward than in the direct experiment. This effectively increases the SNR enhancement.

References

S1. S. Han *et al.*, *J. Magn. Reson.* **182**, 260 (2006).
S2. S. Han, S. Stapf, B. Blümich, *J. Magn. Reson.* **146**, 169 (2000).
S2. D. I. Hoult, R. E. Richards, *J. Magn. Reson.* **24**, 71 (1976).